Team-oriented Adaptive Droop Control for Autonomous AC Microgrids

Qobad Shafiee[1], Vahidreza Nasirian[2], Josep M. Guerrero[1], Frank L. Lewis[2], and Ali Davoudi[2]

[1]Department of Energy Technology, Alborg University, Denmark (qsh@et.aau.dk; joz@et.aau.dk)
[2] Department of Electrical Eng., University of Texas at Arlington, TX USA (vahidreza.nasirian@mavs.uta.edu; lewis@uta.edu; davoudi @uta.edu)

***Abstract*— This paper proposes a distributed control strategy for voltage and reactive power regulation in ac Microgrids. First, the control module introduces a voltage regulator that maintains the average voltage of the system on the rated value, keeping all bus voltages within an acceptable range. Dynamic consensus protocol is used to estimate the average voltage across the Microgrid. This estimation is further utilized by the voltage regulator to elevate/lower the voltage-reactive power (Q-E) droop characteristic, compensating the drop caused by the droop mechanism. The second module, the reactive power regulator, dynamically fine-tunes the Q-E coefficients to handle the proportional reactive power sharing. Accordingly, locally supplied reactive power of any source is compared with neighbor sources and the local droop coefficient is adjusted to mitigate and, ultimately, eliminate the load mismatch. The proposed controllers are fully distributed; i.e., each source requires information exchange with only a few other sources, those in direct contact through the communication infrastructure. A Microgrid test bench is used to verify the proposed control methodology, where different test scenarios such as load change, link failure, and inverter outage are carried out.**

***Index Terms*— AC Microgrid, cooperative control, distributed control, droop control, load sharing, voltage control.**

I. Introduction

As the integration of Distributed Generators (DGs) with power electronic interfaces continues to increase, the concept of Microgrid is becoming more popular [1]–[5]. These local grids are conventionally equipped with a hierarchical control structure to address different control requirements such as frequency and voltage regulation, load sharing, etc. [4], [5]. Primary control is a decentralized approach that provides frequency and voltage regulation. Droop control is widely adopted for the primary control level, which handles (active/reactive) power sharing among sources in proportion to their power ratings [6]–[8].

As sources respond to more power demand, onboard droop controllers reduce their frequency/voltage to handle load sharing and prevent overload/overstress. Identical voltage and frequency measurements are essential to the effectiveness of the droop mechanisms. Unlike frequency which is a global variable, the voltage varies across the Microgrid due to the distribution line impedances. This voltage mismatch incapacitates the droop mechanisms and results in a poor voltage regulation and load sharing.

Centralized secondary controls are conventionally practiced in the literature, e.g., [4]–[5] and [9], to restore the system frequency and voltage. The centralized approach requires point-to-point communication, which adds to system complexity and compromises its reliability. Alternatively, distributed protocols have recently drawn attention for Microgrid control [10]–[13]. Secondary control, in particular, has been the subject of studies in [14]–[16]. The line impedance effect, however, is not taken into account and is still open to research.

This paper introduces a distributed control framework for voltage regulation and reactive power sharing in ac Microgrids. Salient features of the proposed control methodology are outlined:

- Each source carries an embedded secondary control which includes two separate control modules; a voltage regulator and a reactive power regulator.
- The voltage regulator maintains the average voltage amplitude of the Microgrid at the rated value. Dynamic consensus protocol is used in the voltage regulator to estimate the average voltage across the Microgrid.
- The reactive power regulator compares local generation with the neighbors' and, accordingly, adjusts the local droop coefficient to mitigate the mismatch.
- A sparse communication network links the sources (controllers) to exchange control variables. This network must form a connected graph. Additionally, the network shall satisfy a minimum redundancy; the graph remains connected in case of any single link failure. As long as the communication network remains connected, impairments such as delay or packet loss, may not compromise the system performance.
- The control methodology is scalable, for that prior knowledge of the system is not required, as a new component enters the Microgrid.

The reminder of the paper is organized as follows: Section II provides an overview of the distributed control on graphs. The proposed cooperative control framework is introduced in Section III. Section IV discusses the dynamic consensus protocol for average voltage estimation. Section V studies performance of the proposed controller for an ac Microgrid. Section VI concludes the paper.

978-1-4799-4032-5/14/$31.00 ©2014 IEEE

II. Cooperation on Graphs

A distributed network of communication links can connect sources of a Microgrid. Such a cyber network can be represented by a graph, as shown in Fig. 1, where sources and communication links are represented by nodes and edges, respectively. This cyber network facilitates cooperation among agents (sources), where any agent is in contact with only a few other agents as its neighbors, and not with all other agents. This cooperative interaction of the neighbors on the cyber layer sets the ground for the cooperative control, which offers convergence of the control variables (on all nodes) to a global consensus, if the communication graph is properly designed.

The communication graph is a directed graph (digraph) between multiple agents, which is usually represented as a set of nodes $\mathbf{V}_\mathbf{G} = \left\{v_1^\mathrm{g}, v_2^\mathrm{g}, \ldots, v_N^\mathrm{g}\right\}$ connected with a set of edges $\mathbf{E}_\mathbf{G} \subset \mathbf{V}_\mathbf{G} \times \mathbf{V}_\mathbf{G}$ and an associated adjacency matrix $\mathbf{A}_\mathbf{G} = \left[a_{ij}\right] \in \mathbb{R}^{N\times N}$, where N is the number of nodes (sources). The Adjacency matrix $\mathbf{A}_\mathbf{G}$ carries the communication weights, where $a_{ij} > 0$ if $(v_j^\mathrm{g}, v_i^\mathrm{g}) \in \mathbf{E}_\mathbf{G}$ and $a_{ij} = 0$ otherwise. The communication gains, a_{ij} s, can be assumed as data transfer gains. This paper assumes a time-invariant adjacency matrix. $N_i = \left\{j \mid (v_j^\mathrm{g}, v_i^\mathrm{g}) \in \mathbf{E}_\mathbf{G}\right\}$ denotes the set of all neighbors of the Node i. Equivalently, if $j \in N_i$, then v_i^g receives information from v_j^g. However, the links are not necessarily reciprocal, i.e., v_j^g may not receive information from v_i^g. The in-degree matrix $\mathbf{D}_\mathbf{G}^\mathrm{in} = \mathrm{diag}\left\{d_i^\mathrm{in}\right\}$ is a diagonal matrix with $d_i^\mathrm{in} = \sum_{j\in N_i} a_{ij}$. Similarly, the out-degree matrix is $\mathbf{D}_\mathbf{G}^\mathrm{out} = \mathrm{diag}\{d_i^\mathrm{out}\}$, where $d_i^\mathrm{out} = \sum_{i\in N_j} a_{ji}$. The Laplacian matrix is defined as $\mathbf{L} = \mathbf{D}_\mathbf{G}^\mathrm{in} - \mathbf{A}_\mathbf{G}$, whose eigenvalues determine global dynamics of the system. The Laplacian matrix is balanced if the in-degree of each node matches its out-degree, i.e., $\mathbf{D}_\mathbf{G}^\mathrm{in} = \mathbf{D}_\mathbf{G}^\mathrm{out}$. A direct path from v_i^g to v_j^g is a sequence of edges that connects the two nodes. A digraph is said to have a spanning tree if it contains a root node, from which there exists at least a direct path to every other node.

III. Cooperative Control Framework

Each source in a Microgrid has a controller. These controllers are linked through a cyber network. Figure 2 shows the proposed control methodology for a single source, e.g., Source i, which includes two separate modules; voltage regulator and reactive power regulator. The voltage regulator maintains the average voltage of the Microgrid at the rated value, while the reactive power regulator monitors the reactive power sharing and adjusts the droop coefficients to provide proportional load sharing. It should be noted that in a practice, where the line impedances are not negligible, all bus voltages cannot be regulated at identical values, for that it hinders the reactive power management. Typically, the bus voltages are regulated within 95% to 105% of the rated voltage. Accordingly, the proposed method aims to regulate the average voltage of the whole system, rather than individual buses.

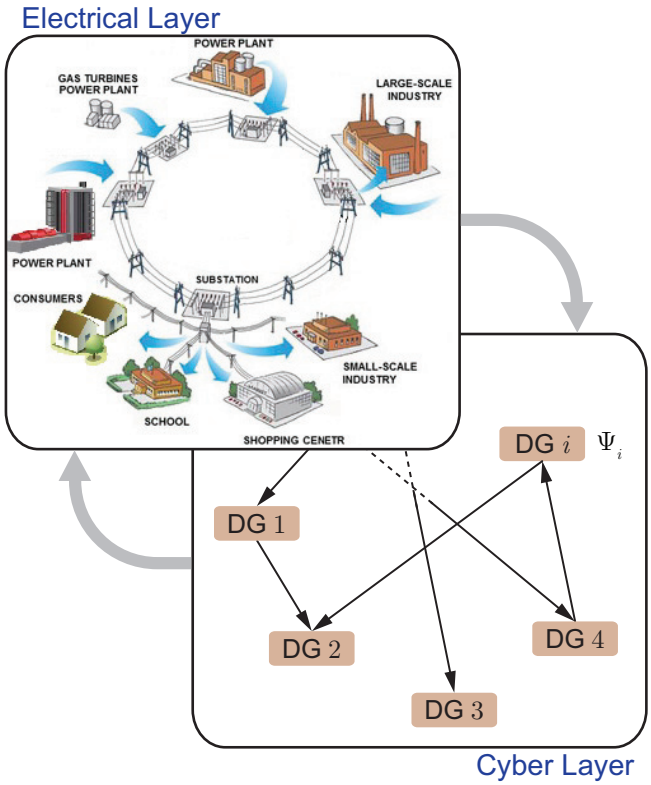

Fig. 1. Layout of an ac Microgrid augmented with a communication network.

The communication network, spanned across the Microgrid, facilitates data exchange among controllers. Each controller, e.g., the controller at Node i, relays an information vector, Ψ_i, to its neighbors on graph. The information vector is formatted as $\Psi_i = \left[\overline{E}_i, Q_i/Q_{i\max}\right]^\mathrm{T}$, where $\overline{E}_i$, Q_i, and $Q_{i\max}$ are the estimate of the average of the voltage amplitudes across the Microgrid, supplied reactive power, and rated reactive power at Node i, respectively. The term $Q_i/Q_{\max}$, which is referred to here as the *loading index*, represents reactive loading percentage of the Source i. Each controller receives data from its neighbors on graph and, through processing local and neighbors' information, it updates its control variables.

A. Distributed Voltage Control

The voltage regulator provides a voltage correction term, δE_i, to boost the voltage amplitude at node i. Each controller has an estimator, highlighted in Fig. 2, that estimates the average of the voltage amplitudes across the Microgrid, $\overline{E}_i$. Functionality of the estimator is explained in details in the subsequent section. The difference between this estimation and the reference voltage amplitude, E^ref, is then fed to a PI controller to calculate the voltage correction term, δE_i. The reference voltage, E^ref, is typically the rated voltage of the Microgrid and, thus, sources share identical reference values. Cooperation among all the voltage regulators guarantees to have the averaged voltage amplitude across the Microgrid regulated at the rated value.

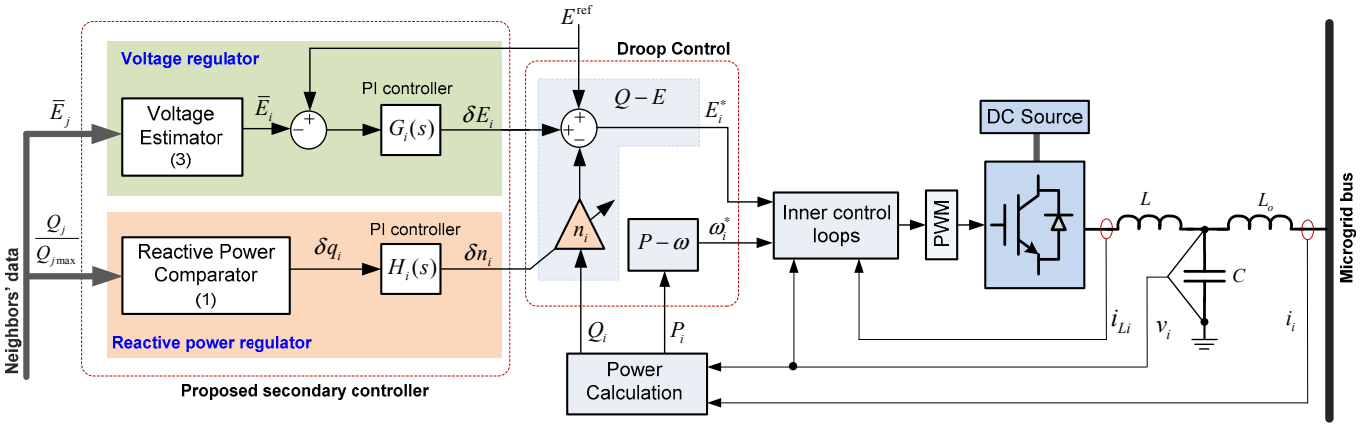

Fig. 2. Cooperative adaptive droop control for the i-th source of an ac Microgrid.

B. *Distributed Adaptive Droop Control*

The reactive power regulator at Node i, receives the loading indices of all its neighbors, i.e., the terms $Q_j/Q_{j\max}$ from all nodes j, $j \in N_i$. Then, it compares its loading index, Q_j, with a weighted average of its neighbors' to calculate the loading mismatch, δq_i,

$$\delta q_i = \sum_{j\in N_i} b a_{ij}\left(\frac{Q_j}{Q_{j\max}} - \frac{Q_i}{Q_{i\max}}\right) = \sum_{j\in N_i} b a_{ij}\left(\frac{Q_j}{Q_{j\max}}\right) - b\left(\sum_{j\in N_i} a_{ij}\right)\frac{Q_i}{Q_{i\max}}. \quad (1)$$

The loading mismatch indicates how far is the reactive power sharing from an ideal sharing scenario, where the whole reactive power is shared among the sources in proportion to their rated power. Accordingly, this term is further used to fine adjust distribution of the reactive powers. As seen in Fig. 2, the loading mismatch, δq_i, is fed to a PI controller to generate the droop correction term, δn_i. This correction term is used to update the droop coefficient,

$$n_i(t) = n_{i0} - \delta n_i(t). \quad (2)$$

where n_{i0} is the initial droop assignment. This adjustment helps to lower the loading mismatch among neighbors' sources and, ultimately, in the whole Microgrid. Equivalently, the loading indices converge to a global consensus, shall the communication graph carry a spanning tree with a balanced Laplacian matrix. Consensus in loading indices satisfies proportional reactive power sharing among sources. It should be noted that the droop correction term, δn_i, must be limited, as large values might affect system stability.

IV. Dynamic Consensus Protocol

The estimator module at Node i (see Fig. 2) provides the average voltage amplitude across the Microgrid.

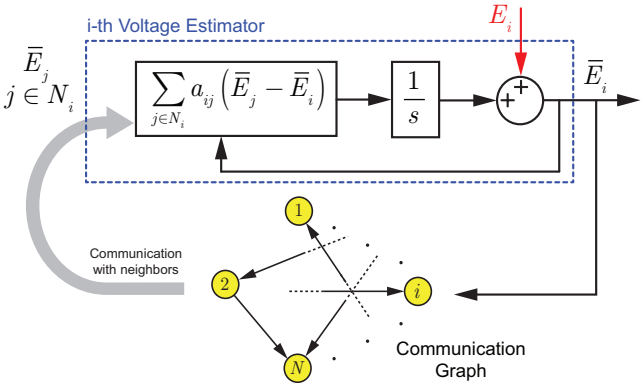

Fig. 3. Dynamic consensus protocol at Node i to averaging the voltage amplitude.

Figure 3 elaborates the so-called *dynamic consensus* protocol which is a distributed decision making approach for estimating the average voltage. Accordingly, the estimator at Node i, updates its estimate based on

$$\bar{E}_i(t) = \int_0^t \sum_{j\in N_i} a_{ij}\left(\bar{E}_j(\tau) - \bar{E}_i(\tau)\right)\mathrm{d}\tau + E_i(t), \quad (3)$$

where E_i is the voltage amplitude at Node i and $\bar{E}_j$ is the estimate of the average voltage amplitude provided by the estimator at Node j. As seen in (3), the updating protocol uses the local voltage, E_i, while no other neighbors measurement is directly fed into the estimation process. Indeed, any voltage variation at any node, e.g., Node i, would immediately affect the estimation at that node, $\bar{E}_i$. Given a connected communication graph, the variation in $\bar{E}_i$ would propagate across the network and affect all other estimations. It is shown in [17] that if the communication graph carries a spanning tree and features a balanced Laplacian matrix, all estimations, i.e., $\bar{E}_i$ s, converge to a global consensus, which is the true average of the voltage amplitudes across the grid. In other words, for each node, the estimated averaged voltage is

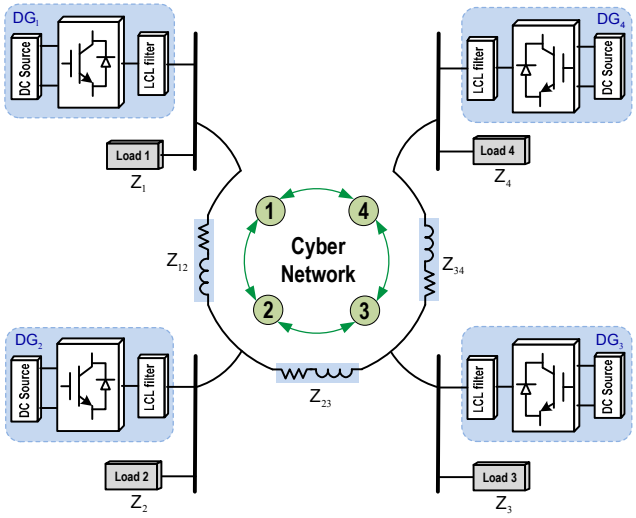

Fig. 4. A 4-bus Microgrid test bench facilitated with cyber network.

$$\lim_{t\to\infty} \bar{E}_i(t) = \frac{1}{N}\sum_{i=1}^{N} E_i(t). \tag{4}$$

V. Case Study

An ac Microgrid test bench, shown in Fig. 4, is considered to study performance of the control methodology. The underlying Microgrid includes four DGs with various rated powers supplying local and distant loads. Rated power of the first two DGs are twice those for the last two. Rated voltage of the system is 230 V with the frequency of 50 Hz. Distribution line impedances are modeled with series RL branches. A communication network, highlighted in green in Fig. 4, facilitates cooperation of the DGs. The links are all bidirectional to feature a balanced Laplacian matrix. It should be noted that alternative cyber structures with less links could also meet the operational requirements. However, a single spare link is considered to 1) improve the system dynamics and 2) maintain graphical connectivity in case of a link/ inverter failure.

The proposed control strategy is simulated in Matlab Simulink®. Associated adjacency matrix of the cyber network, $\mathbf{A}_G$, and the coupling gain between voltage and power regulators, b, are

$$\mathbf{A}_G = \begin{bmatrix} 0 & 2 & 0 & 2 \\ 2 & 0 & 2 & 0 \\ 0 & 2 & 0 & 2 \\ 2 & 0 & 2 & 0 \end{bmatrix}, \quad b = 0.03. \tag{5}$$

Other electrical and control parameters of the underlying system are tabulated in details in Table I. Performance of the cooperative controller is evaluated through subsequent studies:

A. Fixed Droop versus Cooperative Adaptive Droop

Microgrid performance with the proposed control algorithm is compared with the conventional droop control, which uses fixed droop coefficients.

TABLE I
Microgrid Test Bench Electrical and Control Parameters

	Parameters		Value	
	Symbol	Quantity		
Electrical Test System	V_{dc}	DC voltage	650 V	
	E^{ref}	MG voltage amplitude	325 V	
	f	MG frequency	50 Hz	
	C	LCL filter capacitance	25 μF	
	L	LCL filter inductance	1.8 mH	
	L_o	LCL filter impedance	1.8 mH	
	Z_1 , Z_2	Load 1, Load 2	$300 + j314\ \Omega$	
	Z_3 , Z_4	Load 3, Load 4	$150 + j157\ \Omega$	
	Z_{12}	Line impedance 1, 2	$R_{12} = 1.2\ \Omega,\ L_{12} = 5.4$ mH	
	Z_{23}	Line impedance 2, 3	$R_{23} = 0.4\ \Omega,\ L_{23} = 1.8$ mH	
	Z_{34}	Line impedance 3, 4	$R_{34} = 0.4\ \Omega,\ L_{34} = 3.2$ mH	
Control Parameters	Symbol	Quantity	DGs 1 & 2	DGs 3 & 4
	P_{max}	Rated active power	2200 W	1100 W
	Q_{max}	Rated active power	2200 VAr	1100 VAr
	m	$P-\omega$ droop coefficient	0.0008	0.0004
	n	$Q-E$ droop coefficient	0.01	0.02
	k_{pQ}	Q sharing P term	0.01	0.01
	k_{iQ}	Q sharing I term	0.1	0.1
	k_{pv}	Voltage control P term	0.01	0.01
	k_{iv}	Voltage control I term	1.8	1.8

The coefficients are chosen in inverse proportion to the inverters' rated power. Figure 5 shows the results, where for $t < 15$ s the fixed droop controller is effective. Voltage deviation from the rated value can be observed in all voltage amplitudes (see Fig. 5(a)). Moreover, the bus voltages differ because of the line impedance effect, which has clearly affected the efficacy of the reactive power sharing, as seen in Fig. 5(b).

Activation of the proposed controller (see Fig. 5(a)) at $t = 15$ s, boosts all voltages across the Microgrid such that to regulate the average voltage at the rated value, i.e., $\left(\sum_{i=1}^{N} E_i\right)/N = E^{ref}$. The voltage correction terms, δE_i s, are presented in Fig. 5(e). Although the bus voltages are different than the rated voltage, voltage deviations are kept within an acceptable range. This voltage difference is essential to manage the reactive power flow. As it can be seen in Fig. 5(b), fine adjustment of the droop coefficient, using the adaptive droop mechanism, results in accurate reactive power sharing, where the first two sources provide twice as reactive power as the other two do. Droop coefficient adjustment is demonstrated in Fig. 5(c)

Voltage estimator performance is studied in Fig. 5(d). Estimations of the average voltages are plotted in this figure for all controllers. Estimations are compared with the true average voltage amplitude which is the average of the four voltages. An excellent agreement is reported in Fig. 5(d) between the estimations, $\bar{E}_i$ s, and the true average, $\bar{E}$.

B. Transient Response to Load Change

Figure 6 depicts the Microgrid variables during step load changes. The local load at the second bus is unplugged at $t = 15$ s and plugged back in at $t = 20$ s. As seen in Figs. 6(a) and 6(b), global voltage regulation and proportional reactive power sharing are perfectly carried out.

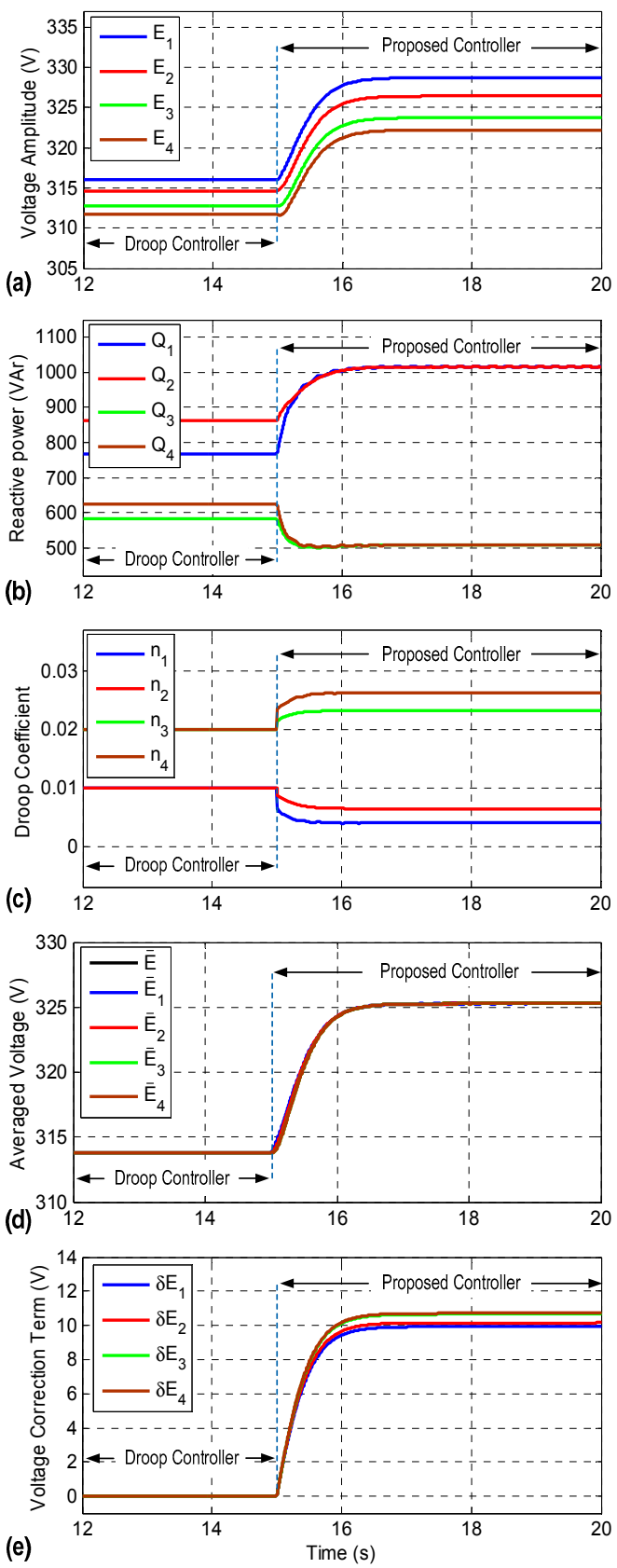

Fig. 5. Performance of proposed controller versus conventional droop control: (a) Bus voltages, (b) Reactive powers, (c) Droop coefficients, (d) Average voltage estimates, (e) Voltage correction terms.

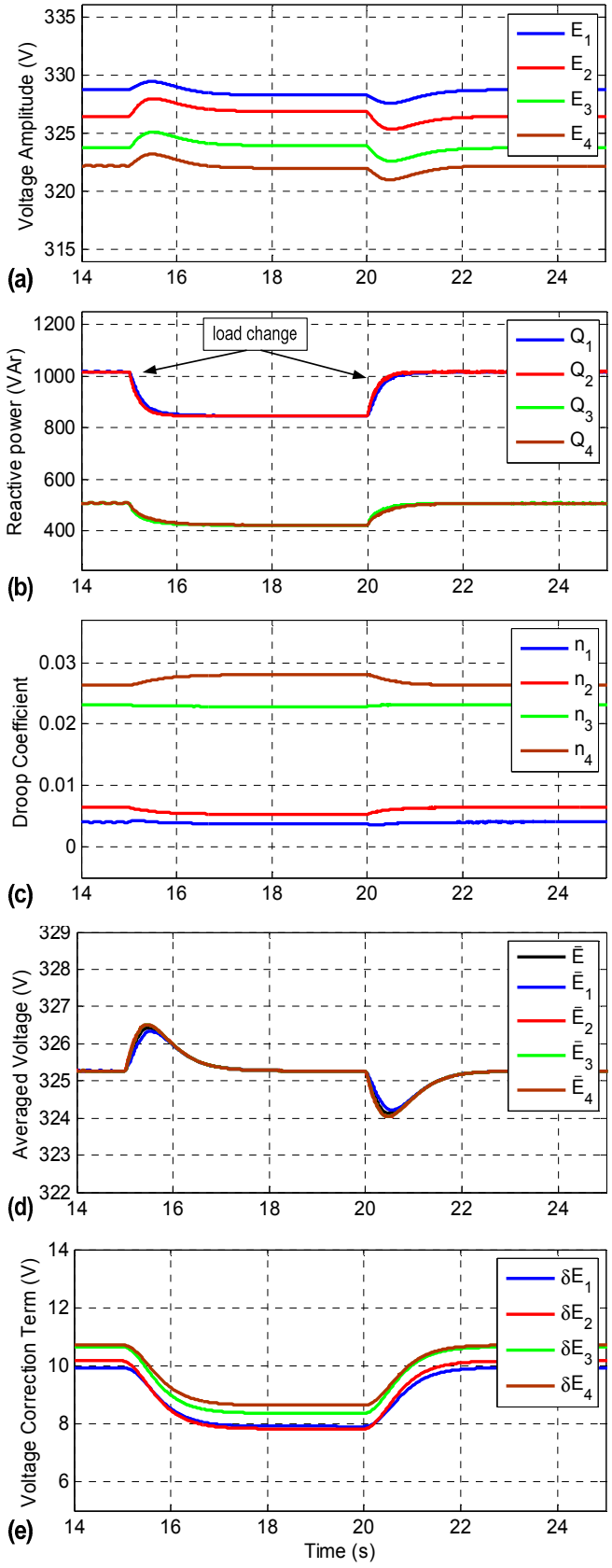

Fig. 6. Performance of the proposed controller in case of a load change: (a) Bus voltages, (b) Reactive powers, (c) Droop coefficients, (d) Averaged voltage estimates, (e) Voltage correction terms.

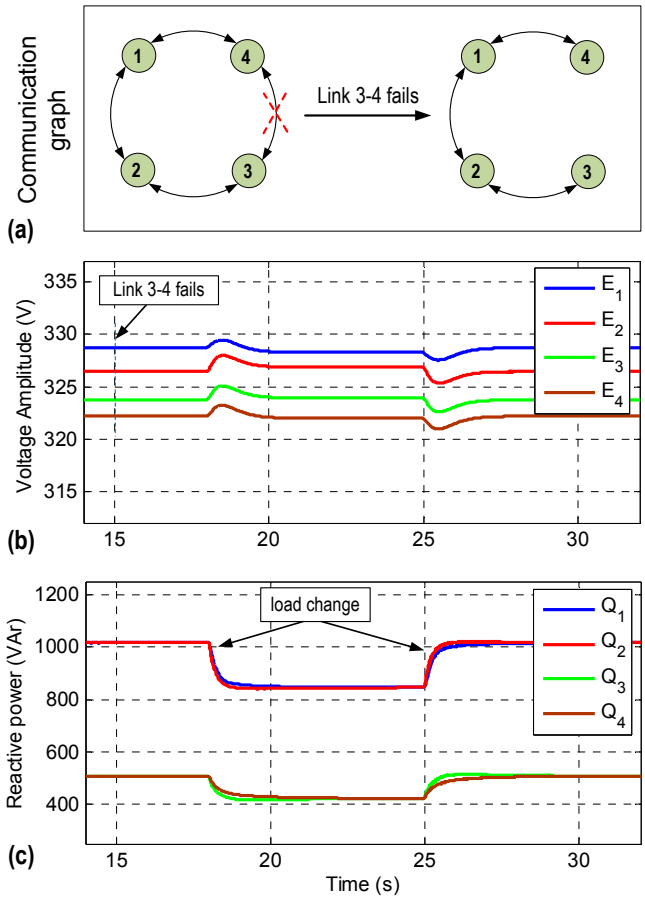

Fig. 7. Communication link failure: (a) Communication graph, (b) Bus voltages, (c) Supplied reactive powers.

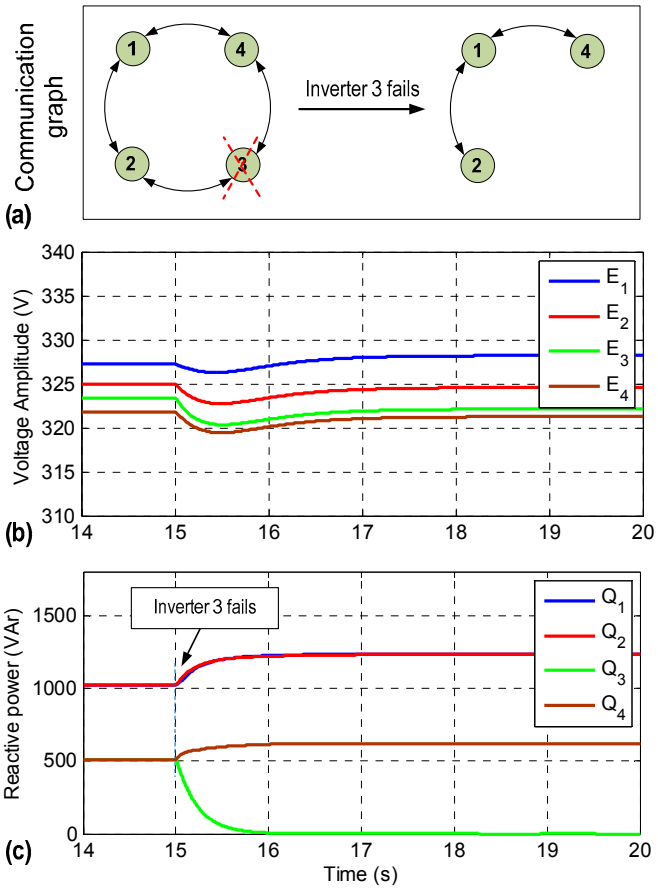

Fig. 8. Inverter failure: (a) Communication graph, (b) Bus voltages, (c) Supplied reactive powers.

Excellent voltage estimation is reported in Fig. 6(d), where the estimations tightly follow true the average voltage, even during transients. Controller response to load change is elaborated in Figs. 6(c) and 6(e), where the droop coefficients, n_is, and voltage correction terms, δE_is, are shown to vary to maintain voltage regulation and proportional load sharing.

C. *Link-Failure Resiliency*

Efficacy of the controller is practiced during a load change with a failed link. The communication link 3-4 (between inverters 3 and 4) is intentionally disabled at $t = 15$ s. As seen in this figure, the link failure does not impact voltage regulation or load sharing in the Microgrid, for that no single link failure does not hinder the graphical connectivity. This concept is illustrated in Fig. 7(a), where it is shown that the graph remains connected when the link 3-4 is disabled. However, any loss of connection affects the Laplacian matrix and, thus, the system dynamic. Generally, less communication links slows down the transient response of the system. Load change is then practiced with the failed link at moments $t = 18$ s and $t = 25$ s. It can be observed in Figs. 7(b) and 7(c) that the voltage regulation and load sharing are successfully handled.

However, comparing Fig. 6(b) and 7(c) implies that the system dynamic has slowed down in Fig. 7(c) due to the loss of a communication link.

D. *Loss of a DG*

Loss of a source (DG) is a common contingency in the Microgrids and, thus, controller performance for such a scenario is subjected to study. Accordingly, the third inverter is intentionally turned off to mimic loss of the third source. It should be noted that, in practice, loss of a source also means the loss of all communication links attached to that particular source. Figure 8(a) illustrates the reconfiguration of the communication network after loss of the third source. It can be see that the network remains connected and, thus, the controller is expected to remain operational. Microgrid voltages and supplied reactive powers are shown in Figs. 8(b) and 8(c) for after the loss of the third inverter, where the global voltage regulation is preserved and the excess reactive power is shared among the remaining sources. It also can be seen that the reactive power supplied to the third bus does not suddenly drop to zero. The slow drop of the reactive power is because of the LCL filter placed between the inverter and the bus.

VI. Conclusion

A cooperative control framework is introduced that handles voltage regulation and reactive power sharing in an ac Microgrid. The Microgrid is augmented with a cyber network for data exchange. Each controller broadcasts an information vector to neighbor controllers, to whom it is directly linked in the cyber domain. Each controller processes local and neighbors' information through two separate modules; the voltage regulator and the reactive power regulator. The voltage regulator features an estimator that estimates the average voltage across the Microgrid. The power regulator dynamically adjusts the local droop coefficient through comparison of the local and neighbors' supplied reactive powers. Comparative studies show that the proposed controller successfully carries out the global voltage regulation and proportional reactive power sharing.

Acknowledgement

This work was supported in part by the National Science Foundation under grants ECCS-1137354 and ECCS-1405173 and by the US Office of Naval Research under grant N00014-14-1-0718.

References

[1] F. Katiraei, R. Iravani, N. Hatziargyriou, and A. Dimeas, "Microgrids management", *IEEE Power Energy Mag.*, vol. 6, no. 3, pp. 54–65, 2008.

[2] J. A. P. Lopes, C. L. Moreira, and A. G. Madureira, "Defining control strategies for Microgrids islanded operation," *IEEE Trans. Power Syst.*, vol. 21, pp. 916–924, May 2006.

[3] F. Katiraei, M. R. Iravani, and P. W. Lehn, "Microgrid autonomous operation during and subsequent to islanding process," *IEEE Trans. Power Del.*, vol. 20, pp. 248–257, Jan. 2005.

[4] J. M. Guerrero, J. C. Vásquez, J. Matas, M. Castilla, L. G. D. Vicuña, and M. Castilla, "Hierarchical control of droop-controlled ac and dc Microgrids—A general approach toward standardization," *IEEE Trans. Ind. Electron.*, vol. 58, no. 1, pp. 158–172, Jan. 2011.

[5] A. Bidram and A. Davoudi, "Hierarchical structure of Microgird control system," *IEEE Trans. Smart Grid*, vol. 3, no. 4, pp. 1963–1976, Dec. 2012.

[6] A. Mohd, E. Ortjohann, D. Morton, and O. Omari, "Review of control techniques for inverters parallel operation," *Elec. Power Syst. Research*, vol. 80, no. 12, pp. 1477–1487, 2010.

[7] Q. C. Zhong, "Robust droop controller for accurate proportional load sharing among inverters operated in parallel," *IEEE Trans. Ind. Electron.*, vol. 60, no. 4, pp. 1281–1290, April 2013.

[8] J. M. Guerrero, J. C. Vasquez, J. Matas, M. Castilla, and L. G. de Vicuna, "Control strategy for flexible Microgrid based on parallel line-interactive UPS systems," *IEEE Trans. Ind. Electron.*, vol. 56, no. 3, pp. 726–736, 2009.

[9] A. Mehrizi-Sani and R. Iravani, "Potential-function based control of a Microgrid in islanded and grid-connected models," *IEEE Trans. Power Syst.*, vol. 25, pp. 1883–1891, Nov. 2010.

[10] J. W. Simpson-Porco, F. Dorfler, and F. Bullo, "Synchronization and power sharing for droop-controlled inverters in islanded Microgrids," *Automatica*, vol. 49, no. 9, pp. 2603–2611, Sept. 2013.

[11] V. Nasirian, A. Davoudi, F. L. Lewis, and J. M. Guerrero, "Distributed adaptive droop control for dc distribution systems," to be published in *IEEE Trans. Energy Convers.*, doi: 10.1109/TEC.2014.2350458.

[12] V. Nasirian, A. Davoudi, and F. L. Lewis, "Distributed adaptive droop control for dc Microgrids," in *Proc. 29th IEEE Appl. Power Electron. Conf. Expo. (APEC),* 2014, pp.1147–1152.

[13] S. Moayedi, V. Nasirian, F. L. Lewis, and A. Davoudi, "Team-oriented load sharing in parallel dc-dc converters," to be published in *IEEE Trans. Ind. Appl.*, doi: 10.1109/TIA.2014.2336982.

[14] A. Micallef, M. Apap, C. Spiteri-Staines, and J. Guerrero, "Secondary control for reactive power sharing in droop-controlled islanded Microgrids," in Proc. *Int. Symp. Ind. Electron. (ISIE)*, 2012, pp. 1627–1633.

[15] Q. Shafiee, J. M. Guerrero, J. Vasquez, "Distributed secondary control for islanded MicroGrids – a novel approach," *IEEE Trans. Power Electron.*, vol. 29, no. 2, pp.1018–1031, Feb. 2014.

[16] A. Bidram, A. Davoudi, F. L. Lewis, and J. M. Guerrero, "Distributed cooperative secondary control of Microgrids using feedback linearization," *IEEE Trans. Power Syst.* vol. 28, no. 3, pp. 3462–3470, Aug. 2013.

[17] V. Nasirian, S. Moayedi, A. Davoudi, and F. L. Lewis, "Distributed cooperative control of dc Microgrids," to be published in *IEEE Trans. Power Electron.*, doi: 10.1109/TPEL.2014.2324579.